



# An experimental test study on ring footing resting on clay bed reinforced by stone column

Shivani Verma<sup>1</sup> · Vikas Kumar<sup>2</sup> · Akash Priyadarshiee<sup>3</sup>

Received: 8 May 2018 / Accepted: 3 August 2018 / Published online: 20 August 2018  
© Springer Nature Switzerland AG 2018

## Abstract

Stone columns are used as a ground improvement technique, and they not only enhance the bearing capacity and reduce the settlement, but also serve as a primary function of reinforcement and drainage. Wrapping the stone columns with geosynthetic materials makes ordinary stone column (OSC) stronger and stiffer by enhancing its performance. Ring footings are more often provided for structures such as storage tanks and bridge piers. Stone column is generally used with square, rectangular and circular footings. The idea of using ring footing with encased stone column is very popular nowadays. By using geosynthetic-encased stone column (GESC) with combination of ring footing, more increase in bearing capacity and reduction in settlement are achieved as compared to OSC. Based on the experimental results, pressure–settlement response of the stone column-reinforced clay was studied. This paper also presents the subgrade modulus aspect of geosynthetic-encased stone column-reinforced clay bed. The aim of this paper is to study the effect of different parameters such as the number of columns, length of column, diameter of column and the effect of encasement provided on OSC and GESC on bearing capacity and on subgrade modulus. The variation of bearing capacity ratio and settlement are also reported for different parameters. The experimental data were further used for regression analysis to fit the equation for bearing capacity of the improved soft clay bed. Thus, it was concluded that with the increase in the number of columns, length and diameter of column, bearing capacity and subgrade modulus of reinforced clay have increased.

**Keywords** Stone column · Ground improvement · Ring footing · Settlement · Bearing capacity · Subgrade modulus

## Introduction

In seismically active region, structures are vulnerable to failure due to excess pore pressure generation and the liquefaction potential of underlying deposits, in the absence of ground improvement techniques [1]. The risk of liquefaction and associated ground deformation can be reduced by various

ground improvement methods such as stone column, lime/cement column and vertical drains. Ground improvement technique such as stone column is a cost-effective solution for structures requiring control on differential settlements. Seismic performance of the stone column is very helpful at sites with liquefaction-induced lateral spreading and in practical engineering applications. Among the various techniques for improving soil conditions, stone columns are most versatile. Stone column is a ground improvement technique to improve load-bearing capacity and settlement of soil. OSCs have been used in wide spectrum of applications for improving the foundation soil properties of rigid and flexible structures such as buildings, embankments and oil storage tanks. In India, the use of stone column began in the early 1970s. Load-bearing columns of well-compacted coarse aggregate are installed in the ground, to serve various purposes such as reinforcement, densification and drainage. They are installed in variety of soils, ranging from loose sands to soft clays and organic soils. Due to their ability to perform a variety of important geotechnical functions, they are most preferred.

---

✉ Shivani Verma  
shivanivermace0094@gmail.com

Vikas Kumar  
vkce@mmmut.ac.in

Akash Priyadarshiee  
i.akashpriyadarshiee1@gmail.com

<sup>1</sup> Seismic Design and Earthquake Engineering, Civil Department, Madan Mohan Malaviya University of Technology, Gorakhpur, Uttar Pradesh 273010, India

<sup>2</sup> Civil Department, Madan Mohan Malaviya University of Technology, Gorakhpur, Uttar Pradesh 273010, India

<sup>3</sup> CED, MIT, Muzaffarpur, India

They mainly provide the function of reinforcement and drainage. Stone columns improve the strength and deformation properties of soft soil in post-installation and reconsolidation phase. They increase the unit weight by replacement and drain quickly the excess pore pressure generated. Stone columns act as a strong and stiff element and carry higher shear stresses. Lee and Pande [2] presented numerical modeling by using a homogenization technique. Stone columns are cost-effective technique for soil improvement. Stone columns are preferred to improve liquefaction resistance of loose sands and to decrease settlement following a seismic event. Ambily and Gandhi [3] reported that a 30-mm sand pad is suitable for stone columns in clay bed. This layer of sand is used to let the foundation distribute load uniformly. When stone column is installed in soft soil, the columns generally fail in bulging due to the lack of lateral support that weak soft soil offers. To overcome this problem, most effective solution is to encase the stone column with a geosynthetic material. Van Impe [4] proposed the idea of encasing the stone column by wrapping with geotextile. Murugesan and Rajagopal [5] and Lo et al. [6] have studied the performance of vertical encased stone columns (VESC) with geosynthetics using numerical models. Gniel and Bouazza [7] studied the effect of encasement on granular columns by triaxial testing and observed increasing strength and stiffness of granular columns due to increasing confining pressure provided by encapsulating reinforcement. Murugesan and Rajagopal [8] performed a series of single and group of load tests with or without encasement using a displacement method. The encasement increases the bearing capacity and the stiffness of soil, prevents squeezing of stones into the surrounding clay, reduces lateral bulging of stone columns and preserves the drainage and frictional properties of stone aggregates. Ghazavi and Afshar [9] performed laboratory tests on stone columns with diameters of 60, 80 and 100 mm and a length-to-diameter ratio of 5. Both unreinforced and encased geotextile-reinforced stone columns were tested. Vertical encased stone column (VESC) has been considered to investigate the effect of reinforcement on the footing load-carrying characteristics. Few experiments were carried out by Chenari et al. [10] on loose sand bed reinforced with stone columns in different patterns, slenderness and area replacement ratios. Performance of the system in terms of both stiffness and bearing capacity was discussed in his research and evaluated both experimentally and numerically. Experiments showed that bearing capacity ratio of the improved system increases with an increase in the number of stone columns in system. Stone column increased the bearing capacity of loose sand by at most 2.75 times. Gniel and Bouazza [11] performed laboratory tests to investigate the efficiency of new alternative method of encasement construction by compression test using different geogrid and stone column aggregates. Ring footings are preferred because of full utilization of soil capacity and less or no tension

condition under the foundation. Ring footings are generally subjected to vertical loads due to the superstructure and the horizontal loads due to the wind pressure acting on the structure. In order to reach maximum bearing capacity from the ring footing, the ratio of inner radius to outer radius should be 0.4. Fisher [12] was the first to study ring foundation behavior. Kumar and Ghosh [13] and Benmebarek et al. [14] have investigated the ultimate bearing capacity and settlements of ring footings. Saha [15] and Saran et al. [16] have performed some experiments to compute the bearing capacity of ring foundations. Sharma and Kumar [17] have performed large direct shear test and drained triaxial shear tests to determine the stress–strain response of ring footing resting on fiber-reinforced and unreinforced sands. Moayed et al. [18] used finite element analysis by ABACUS code and studied the bearing capacity of ring footings on a two-layered soil. Dash et al. [19] have presented the subgrade modulus aspect of geocell-reinforced sand foundation beds. They performed a series of laboratory model tests to determine the subgrade modulus of different parameters, such as the geometry and position of placement of the geocell layer. With the provision of geocell reinforcement, they found that the subgrade modulus of sand bed can be increased as high as eight times compared with the unreinforced case. Bora and Dash [20] have performed experimental tests to investigate the behavior of stone column under load in soft clay bed. The group effect of the stone column was also studied in their investigation. Based on the experimental results, pressure–settlement response of the stone column-reinforced clay was studied. The experimental data were further used for regression analysis to fit the equation for bearing capacity of the improved soft clay bed. Yadav and Tiwari [21] performed different tests as standard Proctor tests, unconfined compressive strength and split tensile strength tests to determine the compaction and strength behavior of cement-stabilized and sodium hydroxide-treated coir fiber-reinforced clay pond ash mixtures. Test results showed that the dry unit weight of the mixtures decreases and water content increases with the addition of pond ash and fibers. The addition of fibers and pond ash in the cementitious clay caused an increase in the unconfined compressive strength, split tensile strength and axial strain at failure. In 2017, Yadav and Tiwari [22] studied the effect of inclusion of waste rubber tire fibers on some of the geotechnical properties of uncemented/cemented clay. For this investigation, three percentages of cement (0%, 3% and 6%) and five percentages of rubber fiber (0%, 2.5%, 5%, 7.5% and 10%) were considered. The experimental test results showed that the incorporation of rubber fiber decreases the unconfined compressive strength and split tensile strength of cement-stabilized clay and modify the rate of loss of post-peak strength and change the brittle failure behavior of cemented clay to ductile. Yadav and Tiwari [23] also studied the compaction and strength characteristics of clayey soil

incorporated with waste crumb rubber and cement for its sustainable use in geotechnical application. Series of unconfined compression strength and split tensile strength tests were carried out on clayey soil incorporated with 3 and 6% of cement by weight and 2.5, 5.0, 7.5 and 10.0% of crumb rubber. It was concluded that crumb rubber up to 5% could be mixed with uncemented or cemented clay soil with the congruent impression. Yadav and Tiwari [24] studied the geotechnical characteristics of cemented clay crumb rubber mixture through a series of compaction, UCS, STS, CBR, one-dimensional consolidation and swelling pressure tests. Crumb rubber and cement content in the mixtures were 0%, 2.5%, 5%, 7.5% and 10%, and 0%, 3% and 6% by the dry weight of the sample. They found that the STS of the composite decreases as the rubber content increases in the cemented clay–rubber mixtures, and with the inclusion of rubber in the cemented clay, the CBR values in unsoaked and soaked conditions decrease; compression index values of the cemented clay–rubber composite were also found to be lower than those of clay. In 2018, Yadav et al. [25] studied the effect of inclusion of pond ash and randomly distributed polypropylene fibers on the strength behavior of cement-stabilized clayey soil. In their investigation, 19 combinations of fiber-reinforced cement-stabilized clayey soil–pond ash mixes at three different percentages of pond ash (i.e., 10, 20 and 30%) and two different percentages of polypropylene fibers (i.e., 0.5 and 1%) of length 6 and 12 mm with 5% cement content were prepared. They concluded that partial replacement of cement-stabilized clayey soil by pond ash with the inclusion of polypropylene fibers causes a significant increase in strength, and decrease in the stiffness and rate of loss of post-peak strength.

## Experimental investigations

Plate load tests were conducted on a model footing resting on clay reinforced with stone columns in a square tank. Tests were performed after reinforcing the soil by introducing the stone columns of 0.16 B and 0.25 B diameter (where B is outer diameter of footing) filled with stone aggregates at different locations. Schematic diagram of model test configuration is presented in Fig. 1a–h. Elevation of the loading platform is shown in Fig. 1i–l. Series of tests were conducted to study the effect of different parameters, related to the bearing capacity and the settlement of reinforced clay. The detail of tests performed is presented in Table 1.

$N_C$	Number of stone columns installed
L	Length of stone column
B	Outer diameter of footing
$D_c$	Diameter of stone column

## Material used

**Soil** A typical clayey soil called kaolin is used in this study. Before test soil was air-dried, basic test was performed. Particle size distribution was obtained by performing wet sieve analysis [ASTM D 6913-04] [26] and hydrometer analysis [ASTM D 4221-99] [27]. The particle size distribution of clay is shown in Fig. 2. Physical properties of clay are presented in Table 2. Around 60% of particles of soil have size less than 0.002 mm. The specific gravity as per ASTM D 0854-06 [28] of clay was found to be 2.66. Atterberg limit tests were conducted as per ASTM D 4318-05 [29], and values of liquid limit, plastic limit and plasticity index were found to be 41.2%, 21.1% and 20.1%, respectively. Thus, the soil is classified as CL (clay with low plasticity) according to Unified soil classification system (USCS) [ASTM D 2487-06] [30].

**Stones aggregate** Stone aggregates with particle size ranging between 4 and 10 mm were used as stone column material (Fig. 3). Particle size distribution curve for stone aggregate is shown in Fig. 4. Water absorption, specific gravity test and other physical properties of aggregates are presented in Table 3.

**Geotextile** Geotextiles are smart and sustainable material for geotechnical and environment application in the whole world. The history of construction and application of geotextile materials backs to 1950s, at which time single-strand woven geotextile sheets were used as a filter for erosion control in state of Florida. Geotextiles are thin structures that can bear the tensile strength but cannot withstand compressive forces. Geotextiles are commonly used to model reinforced soils. For experimental study, non-woven geotextile was used to encase the stone column. Non-woven geotextile was provided by VISHVA MARKETING PVT. LTD. A geotextile sheet of dimension 2 m × 1 m × .5 mm was used for this study. Tensile strength graph of geotextile is shown in Fig. 5. Physical properties of geotextile are presented in Table 4 as per ASTM D4595, 2011 [31].

**Ring footing** Nowadays, more and more ring footings are in practice because they are more economical and decreases the quantity of materials used. Ring footings are most commonly provided for many structures such as bridge piers, transmission towers, silos, water tower structures, chimneys, storage tank. Ring footings are preferred because of full utilization of soil capacity and less or no tension condition under the foundation. Ring footings are generally subjected to vertical loads due to the superstructure and the horizontal loads due to the wind pressure acting on the structure. In order to reach maximum bearing capacity from the ring footing, the ratio of inner radius to outer radius should be 0.4. Ring footing made up of mild steel was used in this study (Fig. 6). The footing with the external and internal diameter of 200 mm and 80 mm and thickness of 10 mm is used.

**Fig. 1** **a** 1 Column at center ( $D_c/B=0.16$ ), **b** 4 columns at  $0.48 B$  distance from center of footing ( $D_c/B=0.16$ ), **c** 5 columns at  $0.32 B$  distance from center of footing ( $D_c/B=0.16$ ), **d** 8 columns at  $0.1875 B$  distance and 1 column at center of footing ( $D_c/B=0.16$ ), **e** 1 column at center ( $D_c/B=0.25$ ), **f** 4 columns at  $0.6 B$  distance from center of footing ( $D_c/B=0.25$ ), **g** 5 columns at  $0.4 B$  distance from center of footing ( $D_c/B=0.25$ ), **h** 8 columns at  $0.1875 B$  distance and 1 column at center of footing ( $D_c/B=0.25$ ), **i** elevation of loading platform for  $N_c=1$ , **j** elevation of platform for  $N_c=4$ , **k** elevation of loading platform for  $N_c=5$ , **l** elevation of loading platform for  $N_c=9$

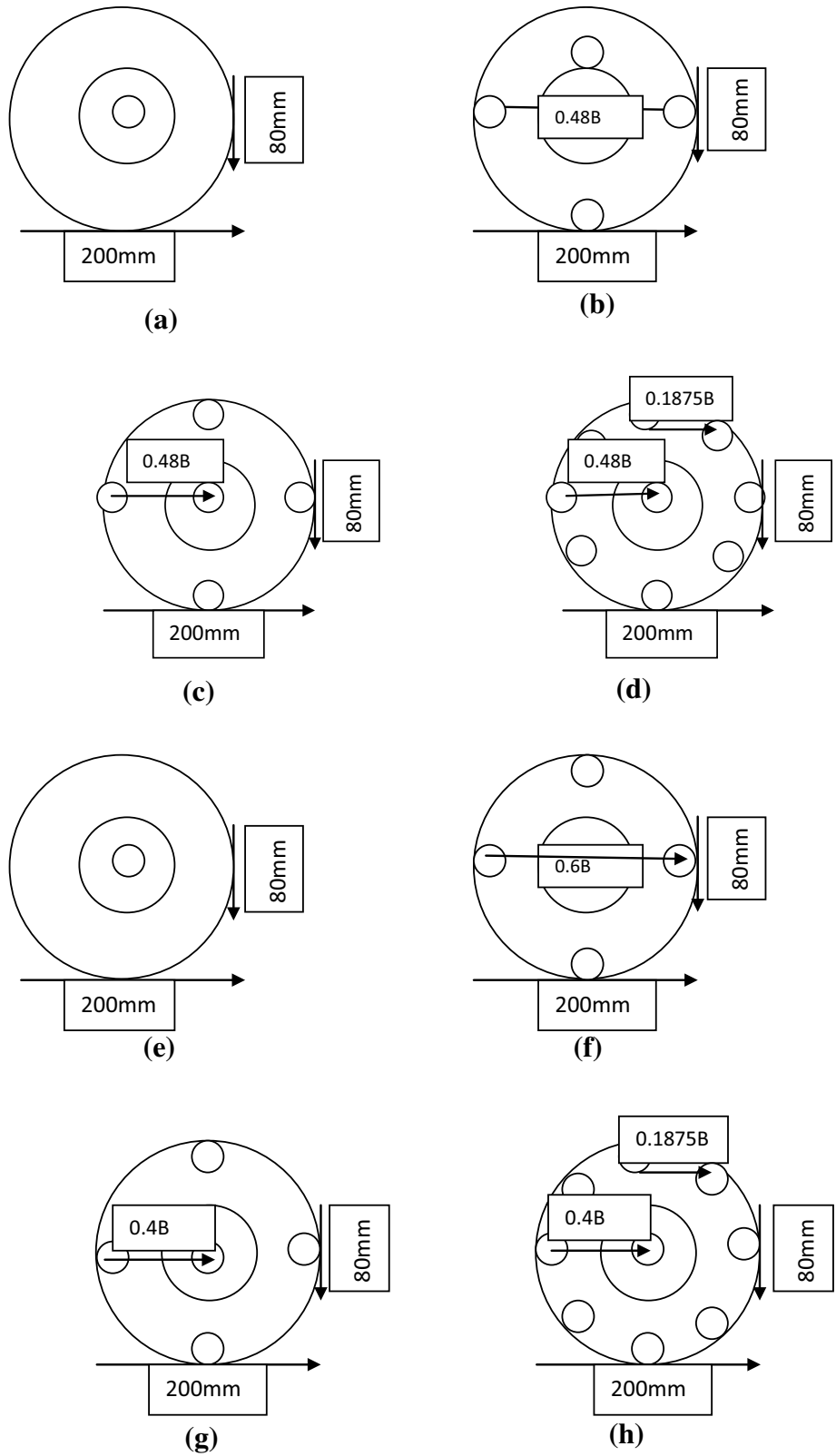
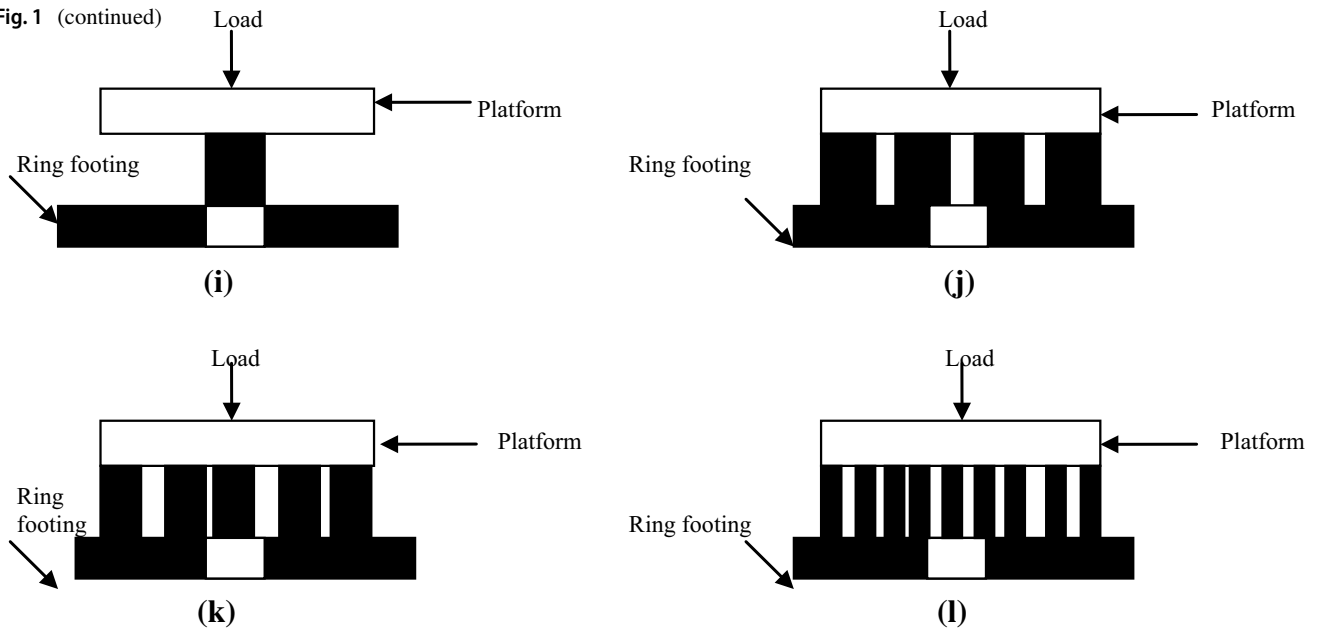


Fig. 1 (continued)



**Table 1** Details of tests performed on soil at  $D_c/B = 0.16$  and  $D_c/B = 0.25$

Effect of parameters	Reinforcement type	Number of column $N_c$	L/B	Dc/B
Number of columns	Unreinforced clay	0	0	0
	OSC	1	1.5	0.16, 0.25
		4	1.5	0.16, 0.25
		5	1.5	0.16, 0.25
		9	1.5	0.16, 0.25
Length of column	GESC	1	1.5	0.16, 0.25
		4	1.5	0.16, 0.25
		5	1.5	0.16, 0.25
		9	1.5	0.16, 0.25
		5	1	0.16, 0.25
Diameter of column	OSC	5	1.5	0.16, 0.25
			2	0.16, 0.25
			1	0.16, 0.25
			1.5	0.16, 0.25
			2	0.16, 0.25
Effect of encasement	GESC	5	1	0.16, 0.25
			1.5	0.16, 0.25
			2	0.16, 0.25
			1.5 ( $L_{enc}/B$ )	0.25
			1.5 ( $L_{enc}/B$ )	0.25

**Preparation of the experimental model**

Soil bed was prepared in a large test box with plan dimensions of 1000 mm × 1000 mm as shown in Fig. 7. The soil bed was prepared in layers, each of which was 50 mm thick. The surface of the box was sealed with a nylon sheet, and the inner face-walls were coated by a thin layer of grease

to reduce the friction between the clay and the tank wall. A uniform compaction effort was done on the surface of each clay layer to achieve uniform required density. The final surface of the clay bed was leveled and trimmed to have a proper thickness and surface in all tests. The same method was used in all tests for the preparation of soil bed. After finishing the top surface of the soil bed, the position

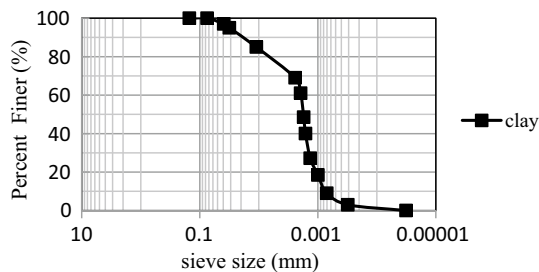


Fig. 2 Particle size distribution of clay

Table 2 Characteristics of soil and values

Specific gravity of soil	2.66
Optimum moisture content	16%
Maximum dry density	17.7 kN/m <sup>3</sup>
Liquid limit	41.2%
Plastic limit	21.1%
Plasticity index	20.1%



Fig. 3 Stone aggregate

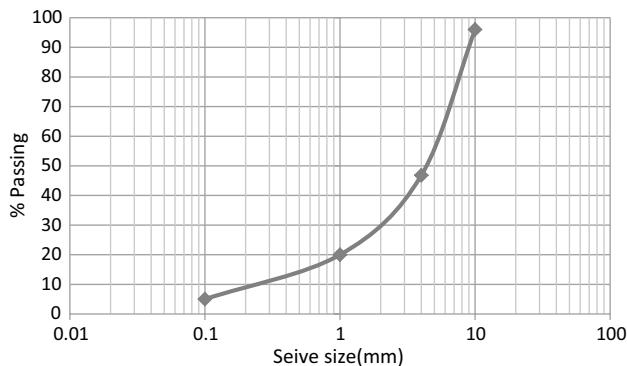


Fig. 4 Sieve analysis of stone aggregate

Table 3 Properties of stone aggregate used

Characteristics	Laboratory values
Density	22.5 kN/m <sup>3</sup>
Water absorption (%)	2.1
Specific gravity	2.6
Maximum dry unit weight (kN/m <sup>3</sup> )	16.64
Minimum dry unit weight (kN/m <sup>3</sup> )	14.13

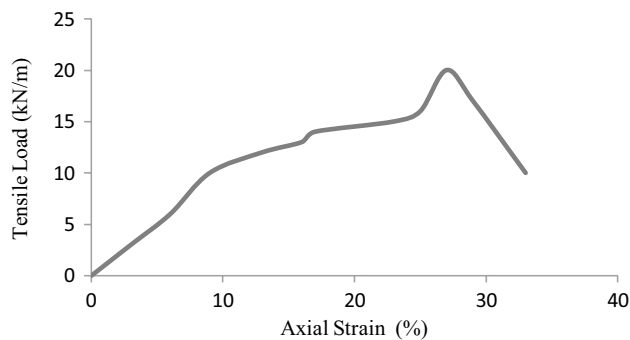


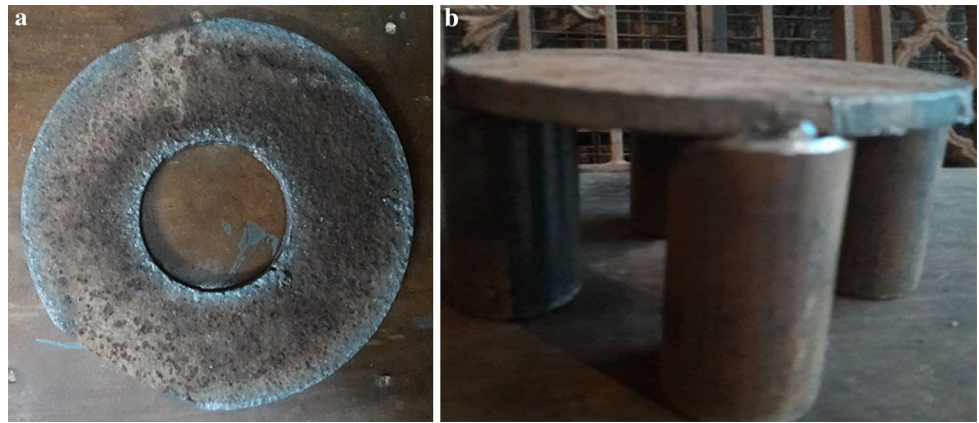
Fig. 5 Tensile strength graph of geotextile

Table 4 Properties of geotextile used

Strength properties	Non-woven geotextile
Base fiber	Polyester
Ultimate tensile strength (kN/m)	20
Strain at ultimate strength (%)	21
Width	1.52 m
Weight	320 gm

of column was marked and casing pipe was pushed into the soft soil at demarcated location. The soil from inside the casing pipe was then taken out with the help of an augur. The pipe was then again pushed into the soil, and the soil was again removed from the pipe. The process continued till the casing pipe to full column length was pushed into the soil. The inner surface of the casing pipe was then properly cleaned off, and then the stone column was casted in steps by compacting the stone chips and withdrawing the casing pipe simultaneously. For encasement of stone column, non-woven geotextile was inserted in the casing pipe of required diameter. The stones were compacted in the same way as earlier. After construction of stone column, sand mat of 200 mm diameter was compressed at a constant strain rate of 1 mm/min to ensure the undrained condition and the corresponding load was observed through a proving ring. The stone column and its tributary soft soil area were loaded through

**Fig. 6** a Ring footing. b Connection between footing and column



**Fig. 7** Test tank



**Fig. 9** Four stone columns



**Fig. 8** 1 Stone column at center



**Fig. 10** Five stone columns

a 10-mm-thick ring footing of external diameter of 200 mm and internal diameter of 80 mm. For ring footings, it was not possible to situate hydraulic jack directly on them because it may slip through the opening of the ring footings. So, to avoid this, first a loading platform was placed on ring footing followed by the hydraulic jack. Then, loading of ring footing

was possible. Figure 1i shows the elevation of loading platform for  $N_c = 1$ , and Fig. 1j shows the elevation of platform for  $N_c = 4$ . Figure 1k shows the elevation of loading platform for  $N_c = 5$ , and Fig. 1l shows the elevation of platform for  $N_c = 9$ . Figures 7, 8, 9, 10, 11, 12 and 13 represent the details of experimental setup and stone columns location.



Fig. 11 Stone column  $D_c/B=0.25 B$  (50 mm)



Fig. 12 Stone column  $D_c/B=0.16$  (32 mm)



Fig. 13 Geosynthetic-encased stone columns

After completion of the test, the stone chips from the column were carefully picked up and a thin paste of plaster Of Paris was poured into the cavity to establish the deformed shape

of the column. The hardened plaster of Paris representing the deformed column shape was isolated by removing the surrounding soft soil (Fig. 13).

## Results and discussion

Laboratory experiments were carried out mainly to observe the influence of some important factors like number of stone column, length of GESC, the diameter of the GESC and encasement on stone column, and on the improvement of the bearing capacity.

### Effect of number of stone columns

Kumar and Kumar [32] have observed that as the number of piles changes, the load-carrying capacity increases. This increase was due to pile that started to interact with the soil across a larger surface area, and thus, load-carrying capacity increased. Figures 14 and 15 show the pressure–settlement curve for different number of vertical columns with different diameters. Results show that as the number of columns increases, bearing capacity of reinforced clay increases significantly. The improvement in bearing capacity takes place up to 42.8% for  $N_c=1$ , 52.5% for  $N_c=4$ , 64% for  $N_c=5$  and 68% for  $N_c=9$  for diameter of stone column  $0.16 B$  and 47.4% for  $N_c=1$ , 58.3% for  $N_c=4$ , 69% for  $N_c=5$  and 74%  $N_c=9$  for diameter of stone column  $0.25 B$ , while keeping  $L/B=1.5$  constant in both cases. As the number of stone columns increases, the lateral bulging of column reduced which increases the bearing capacity of clay bed. Tensile strength of geosynthetic material also plays an important role in reducing the settlement of clay. Also developments of hoop tension force provide additional confining stress which increases the bearing capacity of clay. It is evident from the results that with the number of stone columns varying from 4 to 5, there is substantial improvement in terms of the increase in bearing capacity and reduction in settlement of the reinforced clay bed beyond which ( $N_c=9$ ) further improvement is trivial. So, the number of stone columns giving maximum performance improvement is 5 in both the cases.

### Effect of length of column

Figures 16 and 17 show the variations of pressure–settlement of reinforced and unreinforced clay. Debnath and Dey [33] performed an experimental study on for four different lengths of the stone column as  $L=2 D_c$ ,  $4 D_c$ ,  $6 D_c$  and  $8 D_c$  to determine the effect of length of stone column in the soft clay, and it was found that at  $L/D_c=8$ , optimum improvement in bearing capacity was observed. So in experimental study, we have also kept the same ratio of length to diameter



**Fig. 14** Pressure–settlement curve for ring footing resting on clay reinforced with geosynthetic-encased vertical column at  $L/B = 1.5$  ( $D_c/B = 0.16$ )

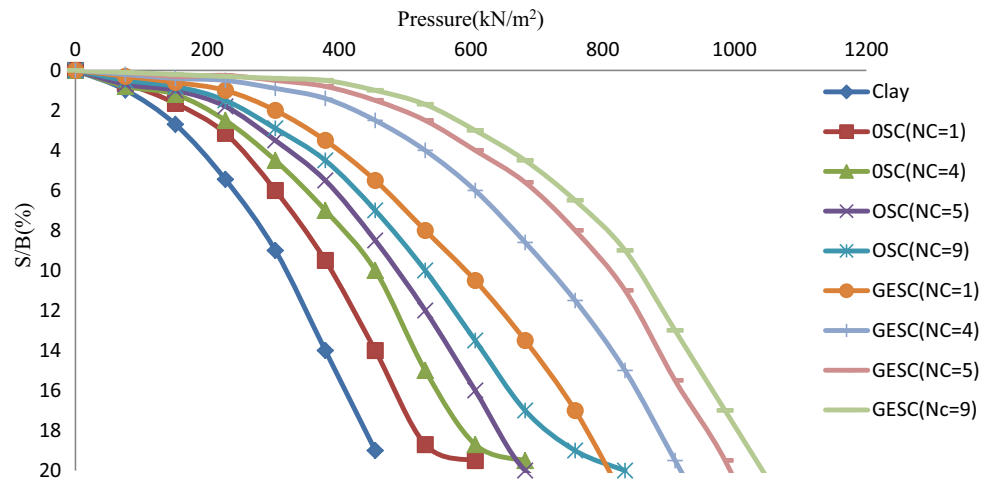


**Fig. 15** Pressure–settlement curve for ring footing resting on clay reinforced with encased vertical column at  $L/B = 1.5$  ( $D_c/B = 0.25$ )

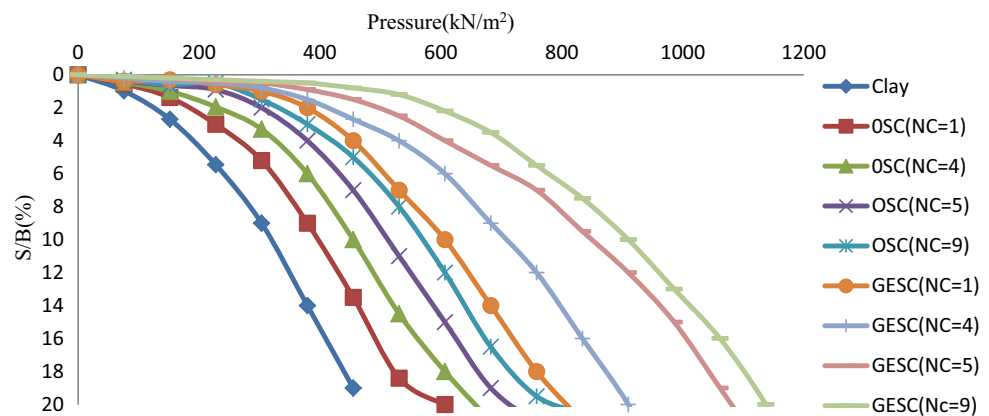
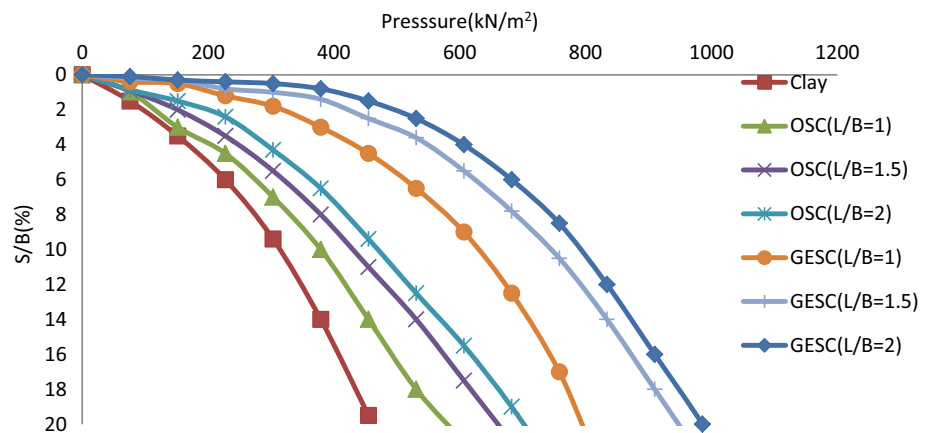


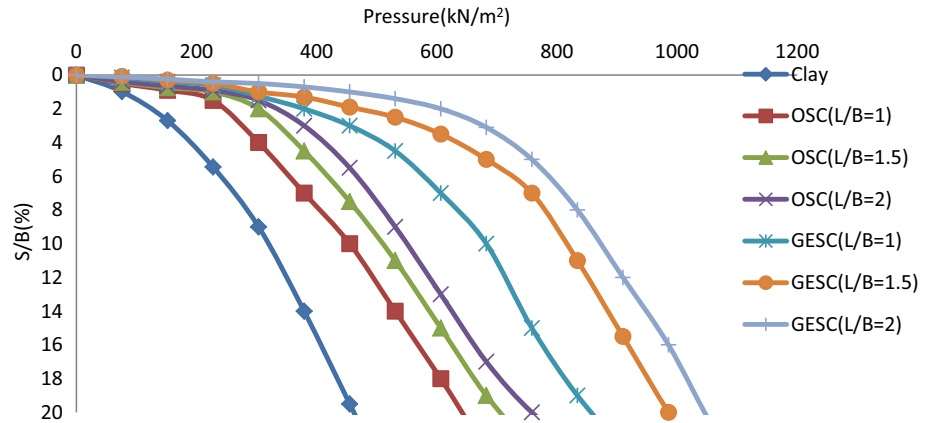
**Fig. 16** Pressure–settlement curve for ring footing resting on clay reinforced with 5 vertical columns ( $D_c/B = 0.16$ )



of stone column as  $L/D_c = 4, 6, 8$  or in terms of diameter of footing, we can represent it as  $L/B = 1, 1.5, 2$ . Results indicate that with the increase in length of column, settlement decreases with reference to settlement of unreinforced clay at the same pressure level. The improvement in bearing capacity takes place up to 65% for  $L/B = 1$ , 73% for  $L/B = 1.5$  and 77% for  $L/B = 2$  for diameter of stone column  $0.16 B$  for 5 number of stone column and 70% for  $L/B = 1$ ,

76% for  $L/B = 1.5$  and 82% for  $L/B = 2$  for diameter of stone column  $0.25 B$  for 5 number of stone column. It could be observed that even with stone column of length as small as ( $L/B = 1$ ), in the clay bed, bearing capacity increases. The performance improvement continues to increase with the increase in length of stone column. It is of interest to note that that with the length of stone column varying from 1 to 1.5 B, there is substantial improvement in terms of the

**Fig. 17** Pressure–settlement curve for ring footing resting on clay reinforced with 5 vertical columns ( $D_c/B=0.25$ )



increase in bearing capacity and reduction in settlement of the reinforced clay bed beyond which when  $L/B=2$  further improvement is trivial. So, length of stone column giving maximum performance improvement in bearing capacity is at  $L/B=1.5$ , or in terms of stone column diameter, it can be said that the optimum length of stone column for  $N_c=5$  is about 6 times the diameter of the column (i.e., 6 dsc).

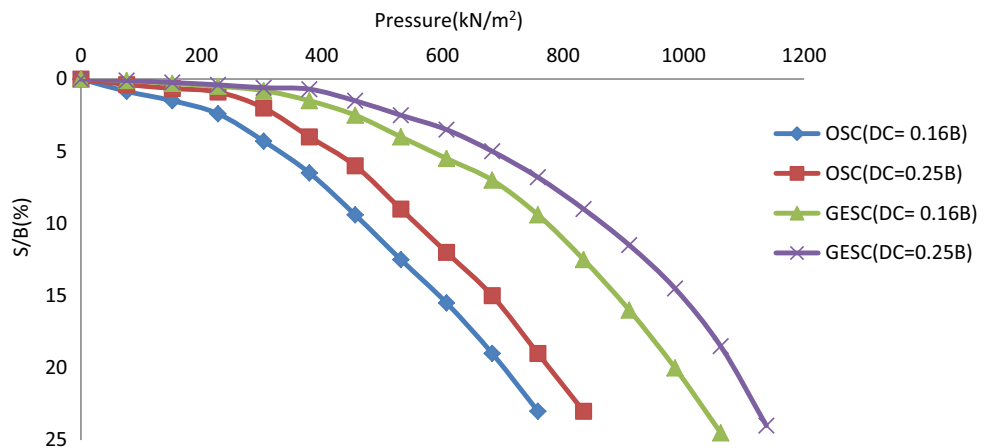
**Effect of diameter of vertical columns**

Figure 18 indicates that with the increase in the diameter of column, bearing capacity increases. The influence of the diameter of the stone column was investigated by performing analyses with diameters of  $0.16 B$  and  $0.25 B$  by applying pressure loading only on the stone column surface, while keeping the  $L/B=1.5$  constant. If diameter of column increases from  $0.16$  to  $0.25 B$ , the increase in bearing capacity is 52–60% for 5 columns. From the result, it is observed that the load-carrying capacity of clay reinforced with stone column of diameter  $0.25 B$  diameters is better as compared to  $0.16 B$  diameter of column.

**Effect of encasement on stone column**

The improvement in the performance of the stone column due to encasement was studied by applying pressure over the stone column of half length encasement ( $L_{enc}/B=0.75$ ) and full length encasement ( $L_{enc}/B=1.5$ ) while keeping length of column constant, i.e.,  $L/B=1.5$ . By encasing, it is observed that the stone columns are confined and the severe lateral bulging has significantly reduced. In case of ring footing, resting on clay bed reinforced by ESCs has undergone much lesser lateral expansion near the ground surface as compared to OSCs. ESCs have undergone slightly higher lateral expansions at deeper depths. This could have happened because the applied surface load is transmitted deeper into the column due to encasement effects. It is clear that the lateral stresses are higher in the fully encased column as compared to the corresponding lateral stresses in clay without reinforcement and half encased column. The increase in confining pressure can be seen over the full height of the stone column, i.e.,  $L_{enc}/B=1.5$ , which leads to the mobilization of higher vertical load capacity in the encased column (Fig. 19).

**Fig. 18** Pressure–settlement curve for ring footing resting on clay reinforced with 5 vertical stone columns ( $L/B=1.5$ )



**Fig. 19** Pressure–settlement curve for ring footing resting on clay reinforced with encased vertical column ( $D_c/B = 0.25$ )

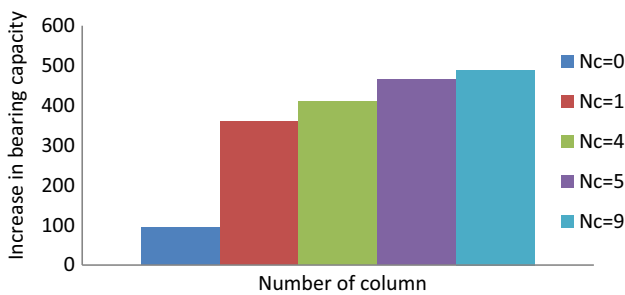
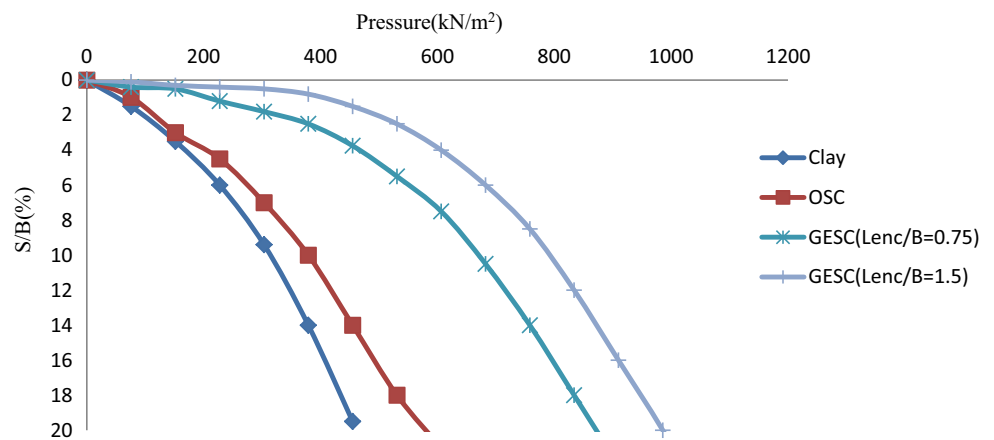


**Fig. 20** Increase in bearing capacity of ring footing resting on clay bed reinforced by geosynthetic-encased stone column due to the number of columns

Figure 20 shows the effect of increasing the number of geosynthetic-encased stone column. It is clear that with increasing the number of columns, in the area below the footing leads to the increase in the bearing capacity. By increasing the number of columns, the horizontal displacement of the column decreases and this reduction in horizontal displacement increases when the column is wrapped with geotextile material and bearing capacity increases significantly.

When the number of columns is 1, bearing capacity is 3.8 times of unreinforced clay. If the number of columns increases from 1 to 4, the increase in bearing capacity values is 4.4 times of unreinforced clay, if the number of stone columns increases from 4 to 5, the increase in bearing capacity values is 5 times of unreinforced clay, and if the number of columns increases from 5 to 9, the increase in bearing capacity is 5.2 times of unreinforced clay that means 5 number of stone column is more effective. From Fig. 20, it is clear that by increasing the number of columns, bearing capacity increases as compared to unreinforced clay. For unreinforced clay, bearing capacity value is very low, but when 1 stone column is installed, bearing capacity value increases due to confinement and shear strength increases. Further increasing the number of GESC to 4, more increase in bearing capacity

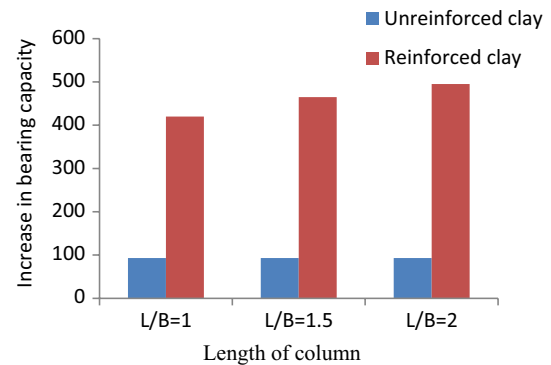


**Fig. 21** Increase in bearing capacity of ring footing resting on clay bed reinforced with geosynthetic-encased stone column due to length of column

is obtained as compared to unreinforced clay. When 5 columns are installed, bearing capacity significantly increases. Similarly, when 9 columns are installed, due to very less spacing between columns improper confinement occurs, but they still reduce horizontal displacement of clay, and therefore, there is an increase in bearing capacity value, but they have not much significant impact on increasing the bearing capacity as compared to the increase in bearing capacity value when 5 columns were installed.

Figure 21 shows the effect of increasing the length of geosynthetic-encased stone column of 0.25 B diameter. Results show that at length  $L/B = 1$ , bearing capacity values is 4.5 times of unreinforced clay, at length  $L/B = 1.5$ , the increase in bearing capacity values is 5 times of unreinforced clay, and further increasing length up to  $L/B = 2$  bearing capacity value becomes 5.3 times of unreinforced clay. With increasing the length of columns, a larger proportion of their full capacity by skin friction is generated and so their full capacity can be mobilized at much lower settlements. Optimum amount of improvement in bearing capacity is obtained at  $L/B = 1.5$ , so length of column,  $L/B = 1.5$  is more efficient than  $L/B = 1$  and  $L/B = 2$  as compared to unreinforced clay;

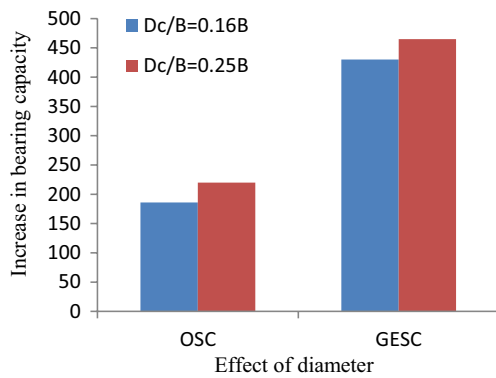


**Fig. 22** Increase in bearing capacity of ring footing resting on clay bed reinforced by geosynthetic-encased stone column due to the increase in diameter of column

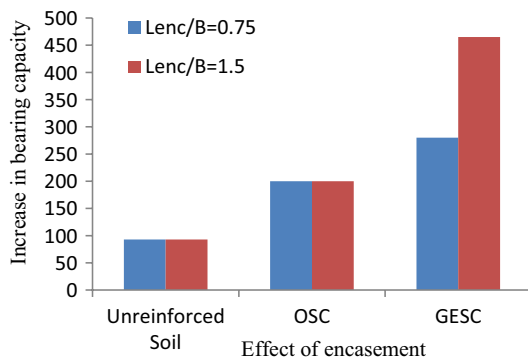
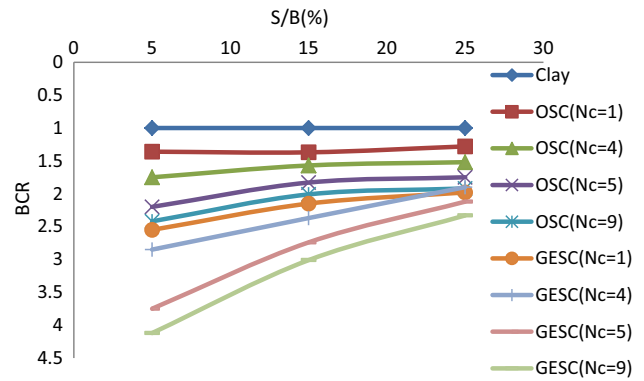


**Fig. 23** Increase in bearing capacity ring footing resting on clay bed reinforced by geosynthetic-encased stone column due to length of encasement

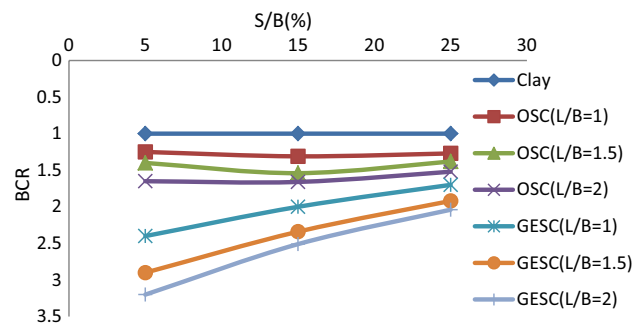
therefore, increasing the length of column of about  $L/B = 1.5$  or 5 times of stone column diameter leads to the increase in the bearing capacity value.

Figure 22 shows the effect of increasing the diameter of geosynthetic-encased stone column. The influence of the diameter of the stone column was investigated by comparing the bearing capacity values of diameters of  $0.16 B$  and  $0.25 B$  with different number of columns while keeping the  $L/B = 1.5$  constant. With the increase in diameter from  $0.16$  to  $0.25 B$ , the increase in bearing capacity is 2.5 times more as compared to OSC for  $N_c = 5$ . In the case of encased stone columns, the performance of  $0.25 B$ -diameter encased stone columns is superior to that of  $0.16 B$  diameter columns. The reason for this is the development of larger additional confining stresses in larger-diameter encased columns as compared to small-diameter column. As size of column increases in confining area under footing, load transfers uniformly under the footing which helps in reducing the settlement of clay.

Figure 23 shows the effect of providing the encasement on stone column in terms of bearing capacity. Result shows



**Fig. 24** Effect of the number of columns on BCR–settlement curve for  $0.25 B$  diameter of stone column at 5, 15, 25% settlement



**Fig. 25** Effect of length of stone column on BCR–settlement curve for  $0.16 B$  diameter of stone column at 5, 15, 25% settlement ( $N_c = 5$ )

that the stone column’ bearing capacity increases by using vertical reinforcing material. Encasing the stone column of full height with geosynthetic material, the load-carrying capacity is improved. The ultimate load and stiffness of the treated clay can be further increased by the use of vertical (VESC) reinforcing material. The bulging failure usually occurs at a depth of  $D$  to  $2D$  from the stone column head (IS: 15284 Part1-2003) [34]. The lateral bulging amount decreases in GESCs as compared with OSCs due to additional lateral confinement provided by geosynthetic material. By encasing OSC of full height with geotextile (GESC), the increase in BCR is 5 times as of unreinforced clay.

Figure 24 represents the BCR values corresponding to 5%, 15%, 25% settlement at  $L/B = 1.5$  for different number of columns. Result shows that with the increase in the number of columns BCR value increases and with increase in settlement BCR value decreases significantly. Figures 25 and 26 represent the effect of length of stone column on bearing capacity ratio (BCR) values corresponding to 5%, 15%, 25% settlement for 5 columns of  $0.16 B$  and  $0.25 B$  diameter and here also, it is evident that at  $L/B = 1.5$  optimum improvement in BCR is obtained. Similarly, Figure 27 represents the effect of increasing

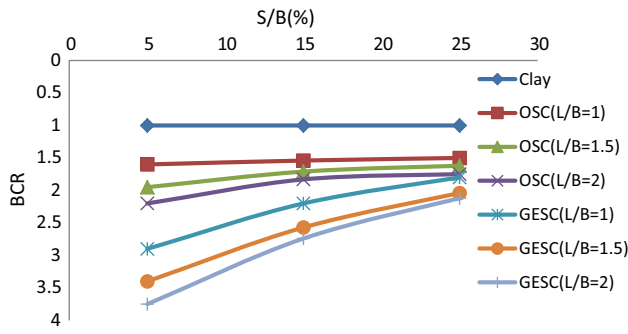


**Fig. 26** Effect of length of stone column on BCR–settlement curve for 0.25 B diameter of stone column at 5, 15, 25% settlement ( $N_c=5$ )

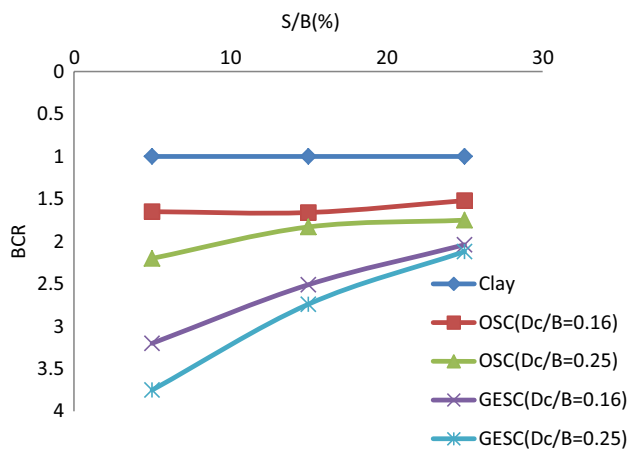


**Fig. 27** Effect of diameter on BCR–settlement curve for  $N_c=5$  at 5, 15, 25% settlement

the diameter of column on bearing capacity ratio (BCR) values corresponding to 5%, 15%, 25% settlement for 5 columns, while keeping  $L/B = 1.5$  constant. Result shows that with increasing the diameter of stone column BCR value increases; however, with increase in settlement, BCR value decreases. Maximum performance in terms of BCR is obtained at 0.25 B diameter of stone column.

### Subgrade modulus

Subgrade modulus is defined as the secant modulus at a point on curve, corresponding to a given settlement where secant is the line joining the point on the curve to the origin. It is also defined as a soil settlement under the certain stress. Hence, modulus of subgrade reaction  $K$  is given by  $P/\delta$ , where  $P$  is the soil bearing pressure and  $\delta$  is the vertical displacement at that point.

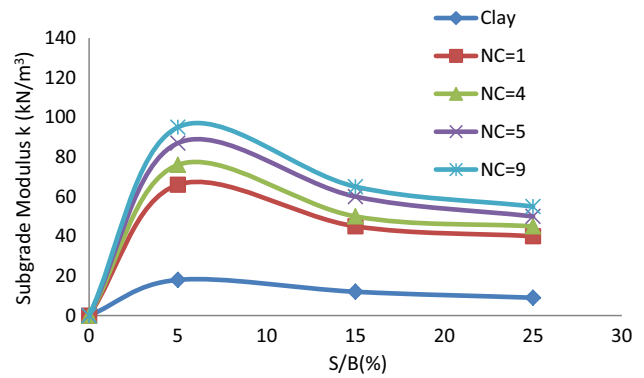


**Fig. 28** Subgrade modulus versus S/B for different numbers of columns ( $D_c/B=0.16$ )

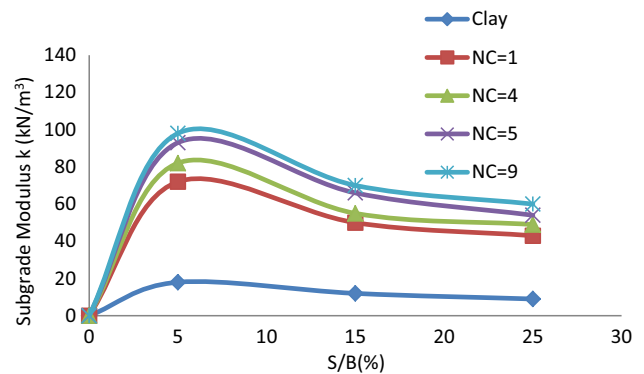


**Fig. 29** Subgrade modulus versus S/B for different numbers of column ( $D_c/B=0.25$ )

### Effect of the number of columns on subgrade modulus

Figures 28 and 29 show the effect of different numbers of columns on subgrade modulus corresponding to 5, 10, 15% settlement at  $D_c/B = 0.16$  and  $D_c/B = 0.25$ . It is observed from the result that with increasing the number of columns, subgrade modulus also increases for both the diameters. For 0–5% range of settlement, the increase in  $k$  value is maximum, further in the range of 5–15%, there is sudden decrease in  $k$  value, and in the range of 15–25% settlement, the decrease in  $k$  value is almost constant. For  $N_c=5$ , there is substantial improvement in subgrade modulus value beyond which ( $N_c=9$ ) further improvement is marginal. Optimum value of Subgrade modulus was obtained at  $N_c=5$  which increased its value by 5.2 times as compared with OSC.

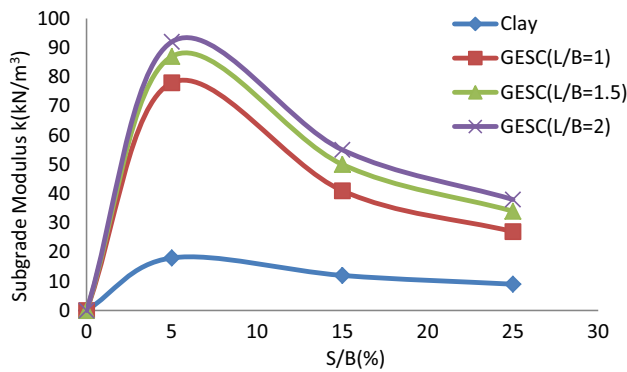


Fig. 30 Subgrade modulus versus S/B for different length of column ( $D_c/B=0.16$ )

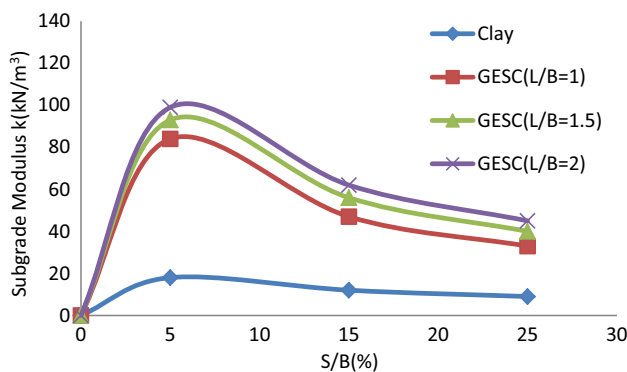


Fig. 31 Subgrade modulus versus S/B for different length of column ( $D_c/B=0.25$ )

### Effect of length of column on Subgrade modulus

Dash et al. [19] have observed that with the increase in height of geocell, subgrade modulus increases; similar kind of result was observed in the case of geosynthetic-encased stone column. Figures 30 and 31 show the effect of length of columns on subgrade modulus corresponding to 5, 10, 15% settlement at  $D_c/B=0.16$  and  $0.25$ , while keeping the number of columns constant ( $N_c=5$ ). It was observed that with increasing the length of column, subgrade modulus increases. For 0–5% range of settlement, the increase in  $k$  value is maximum, further in the range of 5–15%, there is sudden decrease in  $k$  value, and in the range of 15–25% settlement, the decrease in  $k$  value is almost constant. For  $L/B=1.5$ , it is observed that the increase in column length from 1 to 1.5 B leads to a considerable increase in performance; however, with further increase in length from 1.5 to 2 B, the additional improvement is much less. So, optimum improvement in Subgrade modulus is observed at  $L/B=1.5$ . At  $L/B=1.5$ , subgrade modulus increased by 5.2 times as compared with unreinforced case.

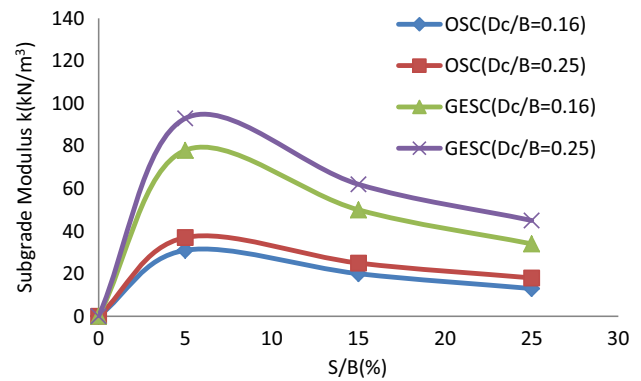


Fig. 32 Subgrade modulus versus S/B for different diameters ( $N_c=5$ )

### Effect of diameter of column on Subgrade modulus

Figure 32 shows effect of diameter of columns on subgrade modulus corresponding to 5, 10, 15% settlement, while keeping the number of columns constant ( $N_c=5$ )  $D_c/b=0.16$ . It is evident from Fig. 32 that diameter of column  $0.25 B$  is more effective as compared to  $0.16 B$  diameter of column. Maximum value of subgrade modulus was obtained at  $D_c/B=0.25$  which increased its value by 3 times as compared with OSC. For 0–5% range of settlement, the increase in  $k$  value is maximum, further in the range of 5–15% there is sudden decrease in  $k$  value, and in the range of 15–25% settlement, the decrease in  $k$  value is almost constant.

### Regression analysis

A multiple variable data regression is performed on the experimental data to establish a relation between the different parameters of stone column and its bearing capacity. It is clear from obtained bearing capacity values that the stone column parameters such as the number of columns ( $N_c$ ), diameter of column ( $D_c/B$ ) and length of column ( $L/B$ ) influence the bearing capacity ( $q_u$ ) [20]. Hence, bearing capacity can be expressed as:

$$q_u = f(N_c, D_c/B, L/B)$$

$$q_u = C_1 * N_c + C_2 * D_c/B + C_3 * L/B + \epsilon$$

where  $\epsilon$ , the error in regression, is the difference between the observed and predicted values of bearing capacity and  $C_1, C_2$  and  $C_3$  are the regression coefficients. The constants  $C_1, C_2, C_3$  are determined by minimizing the sum of squares of the error term over the experimental data. The values obtained from linear regression analysis are:

$$C_1 = 16.5573, \quad C_2 = 484.7533, \quad C_3 = 72.9494, \\ \epsilon = 122.5317 \quad (\text{For GESc})$$

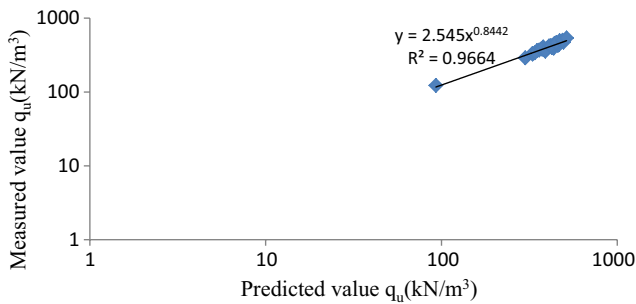


**Fig. 33** Predicted versus measured bearing pressure of geosynthetic-encased stone column-reinforced clay bed

The final form of the proposed model for predicting the bearing capacity of ring footing resting on clay bed reinforced with geosynthetic-encased stone column is expressed by the following equation:

$$q_u = 16.5573 * N_c + 484.7533 * (D_c/B) + 72.9494 * (L/B) + 122.5317$$

The predictive performance of the model is measured through the coefficient of determination ( $R^2$ ). The coefficient of determination ( $R^2$ ) for this model is found to be 0.9, which indicates that the model can predict well. The regression coefficient ( $R^2$ ) is found out to be 0.94. and from Fig. 33, it is observed that the above regression equation predicted can be taken as the best fit for ring footing resting on clay bed reinforced by geosynthetic-encased stone column.

### Conclusion

Based on experimental results, the following conclusions can be drawn.

1. By encasing OSC of full height with geotextile (GESC), the increase in bearing capacity is 5 times that of unreinforced clay.
2. Optimum performance of encased stone column was obtained at 5 columns which increase the bearing capacity of unreinforced clay by 5 times.
3. The length of stone column providing optimum performance improvement is 1.5 B, i.e., 6 times of its diameter.
4. With the increase in diameter of column, ultimate bearing capacity increases. If diameter of column increases from 0.16 to 0.25 B, the increase in bearing capacity is 2.5 times of bearing capacity of OSC.
5. With the increase in the S/B%, BCR reduced for both OSC and GESC; however, with the increase in diameter of column, the number of columns and length of column BCR value increase significantly.

6. Test results have been also used to determine the effect of various parameters on subgrade modulus. Optimum value of subgrade modulus was obtained at  $N_c = 5$  which increased its value by 5.2 times as compared with unreinforced clay, at  $L/B = 1.5$  which increased its value by 5.2 times as compared with unreinforced clay and  $D_c/B = 0.25$  which increased its value by 3 times as compared with OSC.
7. The above predicted regression equation can be taken as best fit to establish bearing capacity of ring footing resting on clay bed reinforced by encased stone column.

**Acknowledgement** I would like to thank my supervised Prof. Vikas Kumar, Civil Department, MMMUT, Gorakhpur, for his direction and consistent support throughout the course of my research work. I genuinely acknowledge and esteem his regarded direction and support from the earliest starting point to the end of my research paper.

### Compliance with ethical standards

**Conflict of interest** On behalf of all authors, the corresponding author states that there is no conflict of interest.

### References

1. Bardet JP et al (1995) The great Hanshin earthquake disaster. In: Preliminary Investigation Report. Department of Civil Engineering University of Southern California, Los Angeles
2. Lee JS, Pande GN (1998) Analysis of stone-column reinforced foundations. *Int J Numer Anal Methods Geomech* 22(12):1001–1020
3. Ambily AP, Gandhi SR (2004) Experimental and theoretical evaluation of stone column in soft clay. In: ICGGE-2004, vol 25, pp 201–206
4. Van Impe WF (1989) Soil Improvement Techniques and Their Evolution. Balkema, Rotterdam
5. Murugesan S, Rajagopal K (2006) Geosynthetic-encased stone columns: numerical evaluation. *Geotext Geomembr* 24:349–358
6. Lo SR, Zhang R, Mak J (2010) Geosynthetic-encased stone column in soft clay: a numerical study. *Geotext Geomembr* 28:292–302
7. Gniel J, Bouazza A (2009) Improvement of soft soils using geogrid encased stone columns. *Geotext Geomembr* 27(3):167–175. <https://doi.org/10.1016/j.geotexmem.2008.11.001>
8. Murugesan S, Rajagopal K (2010) Studies on the behavior of single and group of geosynthetic encased stone columns. *J Geotech Geoenviron Eng ASCE* 136(1):129–139
9. Ghazavi M, Afshar JN (2013) Bearing capacity of geosynthetic encased stone columns. *Geotext Geomembr* 38:26–36
10. Jamshidi Chenari R, Karimpour Fard M, Jamshidi Chenari M et al (2017) Physical and numerical modeling of stone column behavior in loose sand. *Int J Civ Eng* 3:1–14
11. Gniel J, Bouazza A (2010) Construction of geogrid encased stone columns: a new proposal based on laboratory testing. *Geotext Geomembr* 28:108–118
12. Fisher K (1957) Zur Berechnung der setzung Von Fundamenten in der form einer Kreisformigen Ringfläche. *Der Bauingenieur* 32(5):172–174 (in German)

13. Kumar J, Ghosh P (2005) Bearing capacity factor  $N_\gamma$  for ring footings using the method of characteristics. *Can Geotech J* 42(5):1474–1484
14. Benmebarek S, Remadna MS, Benmebarek N, Belounar L (2012) Numerical evaluation of the bearing capacity factor of ring footings. *Comput Geotech* 44:132–138
15. Saha MC (1978) Ultimate bearing capacity of ring footings on sand. M. Eng. Thesis. University of Roorkee, Roorkee
16. Saran S, Bhandari NM, Al-Smadi MMA (2003) Analysis of eccentrically–obliquely loaded ring footings on sand. *Ind Geotech J* 33(4):422–446
17. Sharma V, Kumar A (2017) Strength and bearing capacity of ring footings resting on fibre-reinforced sand. *Int J Geosynth Ground Eng* 3:9. <https://doi.org/10.1007/s40891-017-0086-6>
18. Moayed RZ, Rashidian V, Izadi E (2006) Evaluation on bearing capacity of ring foundations on two layered soil. *World Acad Sci Eng Technol* 61:1108–1112
19. Dash SK, Reddy PD, Raghukanth STG (2007) Subgrade modulus of geocell-reinforced sand foundations. *Proc Inst Civ Eng Ground Improv* 160(G11):1–9
20. Bora MC, Dash SK (2014) Regression model for floating stone column improved soft clay. In: *Proceedings of Indian Geotechnical Conference IGC-2014 December 18–20, Kakinada*
21. Yadav JS, Tiwari SK (2016) Behaviour of cement stabilized treated coir fibre-reinforced clay-pond ash mixtures. *J Build Eng* 8:131–140. <https://doi.org/10.1016/j.jobbe.2016.10.006>
22. Yadav JS, Tiwari SK (2017) Effect of waste rubber fibres on the geotechnical properties of clay stabilized with cement. *Appl Clay Sci* 149:97–110
23. Yadav JS, Tiwari SK (2017) Evaluation of the strength characteristics of cement stabilized clay–crumb rubber mixtures for its sustainable use in geotechnical applications. *Environ Dev Sustain.* <https://doi.org/10.1007/s10668-017-9972-2>
24. Yadav JS, Tiwari SK (2017) A study on the potential utilization of crumb rubber in cement treated soft clay. *J Build Eng* 9:177–191
25. Yadav JS, Tiwari S, Shekhawat P (2018) Strength behaviour of clayey soil mixed with pond ash, cement and randomly distributed fibres. *Transp Infrastruct Geotech.* <https://doi.org/10.1007/s40515-018-0056-z>
26. ASTM Standard D 6913, 2004 (e2) (2004) Standard test methods for particle-size distribution (gradation) of soils using sieve analysis, vol 04.09. ASTM International, West Conshohocken
27. ASTM D 4221-99, 1999 (2005) Standard test method for dispersive characteristics of clay soil by double hydrometer, vol 04.08. ASTM International, west Conshohocken
28. ASTM Standard D 0854, 2006 (2006) Standard test methods for specific gravity of soil solids by water pycnometer, vol 04.09. ASTM International, West Conshohocken
29. ASTM D 4318, 2005 (2005). Standard test methods for liquid limit, plastic limit, and plasticity index of soil, vol 04.08. ASTM International, West Conshohocken
30. ASTM D 2487, 2006 (2006) Standard practice for classification of soils for engineering purposes (Unified Soil Classification System), vol 04.08. ASTM International, West Conshohocken
31. ASTM D4595 (2011) Standard test method for tensile properties of geotextiles by the wide-width strip method. ASTM International, West Conshohocken
32. Kumar V, Kumar A (2018) An experimental study to analyse the behavior of piled-raft foundation model under the application of vertical load. *Innov Infrastruct Solut* 3:35. <https://doi.org/10.1007/s41062-018-0141-8>
33. Debnath P, Dey AK (2017) Bearing capacity of geogrid reinforced sand over encased stone columns in soft clay. *Geotext Geomembr.* <https://doi.org/10.1016/j.geotextmem.2017.08.006>
34. IS: 15284 (Part1-2003) Design and construction for ground improvement—guidelines. Part 1: Stone column ICS 93.020